

Inter-shell interaction in double walled carbon nanotubes: charge transfer and orbital mixing

V. Zólyomi^{1,2}, J. Koltai³, Á. Ruzsnyák³, J. Kürti³, Á. Gali⁴,
F. Simon⁵, H. Kuzmany⁵, Á. Szabados², and P. R. Surján²

¹*Research Institute for Solid State Physics and Optics of the Hungarian Academy of Sciences, P. O. B. 49, H-1525, Budapest, Hungary*

²*Institute for Chemistry, Eötvös University, Pázmány Péter sétány 1/A, H-1117 Budapest, Hungary*

³*Department of Biological Physics, Eötvös University, Pázmány Péter sétány 1/A, H-1117 Budapest, Hungary*

⁴*Department of Atomic Physics, Budapest University of Technology and Economics, Budafoki út 8, H-1111, Budapest, Hungary and*

⁵*Institut für Materialphysik, Universität Wien, Strudlhofgasse 4, A-1090 Wien, Austria*

Recent nuclear magnetic resonance measurements on isotope engineered double walled carbon nanotubes (DWCNTs) surprisingly suggest a uniformly metallic character of all nanotubes, which can only be explained by the interaction between the layers. Here we study the inter-shell interaction in DWCNTs by density functional theory and inter-molecular Hückel model. We find charge transfer between the layers using both methods. We show that not only does the charge transfer appear already at the fundamental level of the inter-molecular Hückel model, but also that the spatial distribution of the change in the electron density is well described already at this level of theory. We find that the charge transfer between the walls is on the order of 0.001 e/atom and that the inner tube is always negatively charged. We also observe orbital mixing between the states of the layers. We find that these two effects combined can in some cases lead to a semiconductor-to-metal transition of the double walled tube, but not necessarily in all cases.

PACS numbers: 71.15.Mb, 73.22.-f, 61.44.Fw

I. INTRODUCTION

Carbon nanotubes have been intensively studied in the past 15 years due to their high application potential and their rich physics. Single walled carbon nanotubes (SWCNTs), in particular, show fundamental phenomena ranging from e.g. possible superconductivity¹ or Luttinger-liquid state² to Peierls distortion³. The electronic properties of SWCNTs are known to be fully determined by their (n, m) chiral indices (which essentially define the alignment of the hexagons on the SWCNT surface with respect to the tube axis)⁴. Peapod annealing produced double walled carbon nanotubes (DWCNTs)⁵ also possess a number of unique properties such as very long phonon and optical excitation life-times⁶. DWCNTs are interacting systems consisting of two subsystems: an inner and an outer SWCNT. The subsystems are still well defined by their (n, m) chiral indices, but lose some of their identity due to the interaction, as suggested by recent experiments. Nuclear magnetic resonance (NMR) measurements show the extremely surprising result that the DWCNTs have a highly uniform metallic character⁷. This observation contradicts theoretical expectations for SWCNTs, especially in the diameter region of the inner tubes, where curvature induces a secondary gap in non-armchair tubes that should be metallic by simple zone folding approximation⁸. Therefore, these NMR observations can only be explained by the interaction between the inner and outer wall. The importance of the interaction is qualitatively easy to understand compared to the case of bundles, where the interaction surface of ad-

acent nanotubes is small, whereas in the case of double walled carbon nanotubes the interaction surface between the two layers is 100 %. Resonant Raman measurements have previously given experimental evidence for the redshift of the Van Hove transition energies due to the interaction between the layers in DWCNTs, as well as for a dependence of the redshift on the inter-shell distance⁹.

In this work we present the results of our theoretical investigation of inter-shell interaction and its consequences in DWCNTs. We studied 65 different DWCNTs by inter-molecular Hückel (IMH) model^{10,11}. We have also studied 6 of these DWCNTs – 3 commensurate $(n, n)@(n', n')$ and 3 commensurate $(n, 0)@(n', 0)$ DWCNTs – by first principles density functional theory within the local density approximation (LDA). We found a semiconductor-to-metal transition in 2 of the 3 $(n, 0)@(n', 0)$ DWCNTs studied by DFT, with only the third one retaining a small band gap. We have previously reported that our calculations predict a large density of states at the Fermi-level in the case of metallic non-armchair DWCNTs, and that starting from two semiconducting SWCNTs the resulting DWCNTs may transform into a metallic state, but not necessarily in every case¹². In Ref.¹², we briefly outlined some of the results of the present paper, namely that a small charge transfer (CT) from the outer wall to the inner wall occurs in every DWCNT. This effect has since been confirmed by photoemission spectroscopy¹³. Here we present our results on the charge transfer in full detail. We point out that the spatial distribution of the change in the electron density according to the inter-molecular Hückel model is in excellent agreement with

first principles calculations in the case of the most typical inner diameters, pointing out that the interactions are well described already at this simple fundamental level of theory. We also find orbital mixing between the layers, which can explain the measured redshift of the resonance in the Raman measurements of DWCNTs⁹. We conclude that the observed charge transfer and orbital mixing together can account for a semiconductor-to-metal transition of DWCNTs, but not necessarily a near-universal metallicity.

II. METHOD

LDA calculations were performed both with a plane wave (VASP¹⁴) and a localized basis set (SIESTA¹⁵) package. In the VASP calculations the projector augmented-wave method was applied using a 400 eV plane-wave cutoff energy, while in the SIESTA calculations double- ζ plus polarization function basis set was employed. 16 irreducible k -points were used; comparison with test calculations using 31 k -points showed this to be sufficient. As these codes use periodic boundary conditions, only commensurate DWCNTs can be studied by them in practice. Otherwise, a model of incommensurate DWCNTs would require huge supercells. An alternate approach to compare the inter-shell interaction in different DWCNTs is the inter-molecular Hückel (IMH) model^{10,11}. In this case the tight binding wave functions originate from the inner and outer tubes (orbital mixing). Using a Lennard-Jones type expression to account for inter-cluster interactions, the tight binding model has been applied to characterize weakly interacting carbon nanotubes^{16,17,18,19}. The tight binding principle can be generalized to apply to both intra- and inter-molecular interactions^{20,21,22}, leading to the IMH model¹⁰, which has been successfully applied to study DWCNTs¹¹ and bundles of SWCNTs²³. Detailed account of the model is given in Ref.²³. The IMH model allows to calculate the charge transfer (CT) for *any* DWCNT with good efficiency. Test calculations on the commensurate (7,0)@(16,0) DWCNT show, that the infinite limit is easy to obtain from calculations on finite DWCNT pieces of gradually increasing length, and the error is less than 0.2 %. Furthermore, optimizing the bond lengths by means of the Longuet-Higgins-Salem model^{24,25} prior to the CT calculations, the charge transfer is altered by merely 0.8 % as compared to the graphene wrapping model, showing that the CT is not very sensitive to the actual bond lengths at this level of theory.

III. RESULTS

The DWCNTs considered in our calculations were selected based on Raman measurements⁹. The experimental diameter distribution of the outer wall of the DWCNTs was centered at 1.4 nm with a variance of 0.1 nm

while the ideal diameter difference between the inner and outer wall is 0.72 nm with a variance of 0.05 nm, corresponding to an inner diameter distribution centered at 0.68 nm. The Raman measurements clearly show that there is no chirality preference for the inner-outer tube pairs and a wide range of combinations can be found in the sample. In accordance with this, we have chosen to examine the inner tubes which are at the center of the inner diameter distribution, and to examine each inner tube with various outer tubes, in order to examine the chirality-dependence of the interactions. In the case of the IMH calculations, the diameter of each tube was taken from the usual graphene folding formulas with a uniform bond length of 1.41 Å, while in the case of the LDA calculations we used optimized geometries²⁶. All inner tubes with diameters $d_{inner} = 0.7 \pm 0.05$ nm were examined, and for each inner tube all outer tubes with diameters $d_{outer} = d_{inner} + 0.72 \pm 0.04$ nm were considered yielding a total of 60 different DWCNTs. In addition we have also studied five other DWCNTs which are outside of the aforementioned diameter range, but could still be present in the sample, in order to compare with the LDA calculations. The 6 commensurate DWCNTs studied by LDA were: (4,4)@(9,9), (5,5)@(10,10), (6,6)@(11,11), (7,0)@(16,0), (8,0)@(17,0), and (9,0)@(18,0).

We calculated the band structure of the 6 commensurate DWCNTs by both LDA packages, and found fairly good agreement between localized basis set calculations and well-converged plane wave results. The three armchair DWCNTs are all metallic, exactly as expected. Of the three zigzag DWCNTs, (8,0)@(17,0) remains a semiconductor, while the other two are metallic. Note, that all zigzag SWCNTs considered were originally semiconducting: the LDA gaps of (7,0) and (16,0) were 0.21 eV and 0.54 eV, respectively, while those of (9,0) and (18,0) were 0.096 eV and 0.013 eV, respectively⁸. The LDA band gap of (8,0)@(17,0) is about 0.2 eV which is much smaller than that of the individual SWCNTs of about 0.6 eV⁸. The band structures of the (7,0)@(16,0) and (8,0)@(17,0) DWCNTs are plotted in Figure 1.

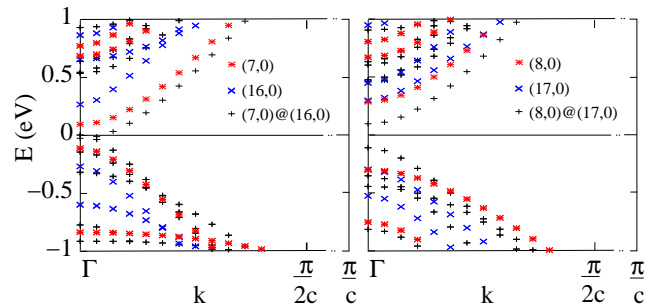


Figure 1: LDA band structures of the (7,0)@(16,0) and (8,0)@(17,0) DWCNTs, in comparison with the band structures of their subsystems in isolated single geometry (the Fermi levels are all shifted to 0 eV).

An earlier study of a linear carbon chain in SWCNT²⁷

indicates that metallicity may occur due to charge transfer between the layers of the DWCNT. To investigate the reasons for metallicity in more detail, we have calculated the CT in the 65 DWCNTs in the IMH model. This is straightforwardly determined by summing up the contributions of the LCAO-coefficients of every occupied molecular orbital separately for the atoms in the inner and outer wall, and then comparing with the number of electrons that should be present on the given wall if there was no CT. Figure 2 shows our results for the charge transfer density along the tube axis as a function of the difference between the inner and outer diameter ($\Delta d = d_{outer} - d_{inner}$). In all cases, we found that the inner tubes are negatively charged. This result is in perfect agreement with recent observations of photoemission spectra of DWCNTs, which also predict negatively charged inner tubes¹³. Our calculated values for the CT density were between $0.005 \text{ e}/\text{\AA}$ and $0.035 \text{ e}/\text{\AA}$. This corresponds to a range of about 0.0005 to $0.0045 \text{ e}/\text{atom}$ for the inner wall, and 0.0002 to $0.0024 \text{ e}/\text{atom}$ for the outer wall; note, that this CT is much smaller than what is typical in e.g. alkali-intercalation experiments. While the CT values show a decent amount of scattering, there is also a strong and clear overall decrease of the CT as Δd increases, which is expected, as the overlap between the orbitals of the two separate layers decreases as the distance between them increases. The large variance of the points is related to the difficulty of accurately predicting a CT of this order of magnitude. However, it is safe to conclude, that the CT density in units of $\text{e}/\text{\AA}$ can be estimated by the linear formula $-0.028 \cdot \Delta d + 0.219$ with a considerable variance depending on tube chirality.

Advancing beyond the IMH model, we calculated the charge transfer for the six commensurate DWCNTs by LDA. In the case of the plane-wave calculation, we were able to calculate the Bader-charges with Voronoi partitions (which defines the borders of the atomic volumes by planes half way between atoms, similar to the construction of Wigner-Seitz cells) using an external utility²⁸. In the case of the localized basis set calculation, Mulliken population analysis could be performed. We found, that the direction and the order of magnitude of the CT is the same in these cases as what was found with IMH. The LDA CT is however somewhat smaller. This is illustrated in the inset of Figure 2. Note, that the Bader charges agree very well with the Mulliken charges. This is not necessary to occur, as the Mulliken population analysis usually only performs well in minimal basis set, however, if all atoms are of the same species (like in our case) then a larger basis set can also give reliable Mulliken charges, and apparently such is the case in our calculations.

Based on the good agreement between the three different CT calculations, we conclude that in DWCNTs electrons are transferred from the outer to the inner wall on the order of 0.005 to $0.035 \text{ e}/\text{\AA}$, depending on tube chiralities.

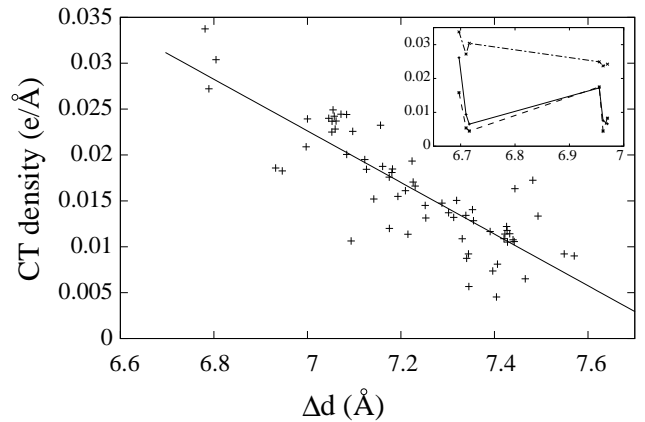


Figure 2: Charge transfer density along the tube axis versus the diameter difference (Δd) between the inner and outer tube according to the IMH model. The straight line is a linear $a \cdot \Delta d + b$ regression (see text). The inset shows a comparison between IMH and LDA results. The CT values obtained from the VASP calculations by analyzing the Bader charges (dashed) agree well with those obtained from the SIESTA calculations by Mulliken population analysis (solid), but both of them give a smaller value than the IMH method (dashed-dotted). The 6 points of each calculation correspond to $(4,4)@(9,9)$, $(5,5)@(10,10)$, $(6,6)@(11,11)$, $(7,0)@(16,0)$, $(8,0)@(17,0)$, and $(9,0)@(18,0)$, from left to right.

IV. DISCUSSION

We found for the 3 commensurate $(n,0)@(n',0)$ DWCNTs that, due to the small magnitude of the charge transfer, the Fermi level is close to the Van Hove singularities that used to form the band gap of the single walled subsystems. This results in a large density of states at the Fermi level¹², very similar to the case of chain@SWCNT systems²⁷. Based on our IMH results, which say that the chirality-dependence of the magnitude of the CT is more-less uniform, we can safely conclude that this large density of states at the Fermi level is expected in all of those metallic DWCNTs, where at least one of the two subsystems is a non-armchair tube, as all but armchair tubes have Van Hove singularities near the Fermi level at diameters above 0.5 nm ⁸. Thus we expect that the majority of the metallic DWCNTs have a large density of states at the Fermi level. This behavior is very similar to doped multi-walled tubes, which have previously been suggested as possible future superconductors¹.

The case of the non-metallic $(8,0)@(17,0)$ DWCNT deserves attention. The two subsystems are semiconducting having almost the same band gap ($\approx 0.6 \text{ eV}$) at LDA level⁸. The DWCNT they form remains semiconducting, but the bands near the Fermi level are distorted as compared to the rigid band prediction, such that the band gap drops to $\approx 0.2 \text{ eV}$. This result underlines the importance of orbital mixing, and points out that the interaction between the inner and outer tubes is not limited merely to charge transfer, but the mixing of inner and

outer tube orbitals is also an important part of the interaction. Furthermore, this result also shows that the orbital mixing caused by the inter-shell interaction provides the explanation to the experimentally observed redshift of the Van Hove transition energies⁹. The redshift is immediately understood by the contraction of the bands such as in the case of (8,0)@(17,0) in Figure 1. In the experiments, all Van Hove transition energies show a redshift, with the lower energy transitions of a DWCNT suffering a greater shift than its higher energy transitions; our calculations show exactly the same qualitative trend.

Thus, from the point of view of the electronic states, a DWCNT should – strictly speaking – always be considered as one single unified system. Approximating a DWCNT by separating it to an inner and an outer subsystem is definitely possible, but it should always be done with caution. For example, if orbital mixing were small, one could estimate whether a given SWCNT is likely to become metallic as one layer of a DWCNT, by calculating the critical charge transfer (CT_{crit}) – the CT where the isolated tube becomes metallic upon doping – for the charged, isolated SWCNT. However, this method is not reliable for DWCNTs, because it completely neglects orbital mixing, which is obviously an important factor, as detailed above. In fact, we have calculated CT_{crit} for the two subsystems of the (8,0)@(17,0) DWCNT with this method, and in both cases we obtained a value which is about a factor of 2 *smaller* than the CT from the DWCNT calculation. This contradictory result clearly shows that the question of whether a given DWCNT is metallic cannot be answered by means of calculating CT_{crit} on charged SWCNTs.

Another reason why it is not trivial to separate the two subsystems is the delocalized profile of the spatial distribution of the change of the electron density induced by the inter-layer interaction, which we will refer to as the charge redistribution profile. It has been pointed out in previous works in the local density approximation, that upon examining the contour plots of the change of the electron density in DWCNTs, it could be found that the electrons deplete from the walls and accumulate in the space between the layers^{29,30,31}. We have also performed these calculations on the charge redistribution profile for the DWCNTs we examined, and found good agreement with these previous works (see below). These results suggest that it is very difficult to divide the charges of the total charge density between the layers. Experiments however show that the layers behave more-less individually, as e.g. Van Hove transitions of the inner and outer tubes can be clearly identified in Raman measurements⁹. Furthermore, recent measurements clearly identify an inter-layer charge transfer in DWCNTs¹³, as mentioned earlier. We have used 3 different methods to calculate the charge transfer between the layers, and all 3 methods showed good agreement with the experimentally observed direction of the charge transfer. This shows that the charge transfer analyses we conducted are able to perform a plausible separation of the charge density between the

inner and outer nanotube.

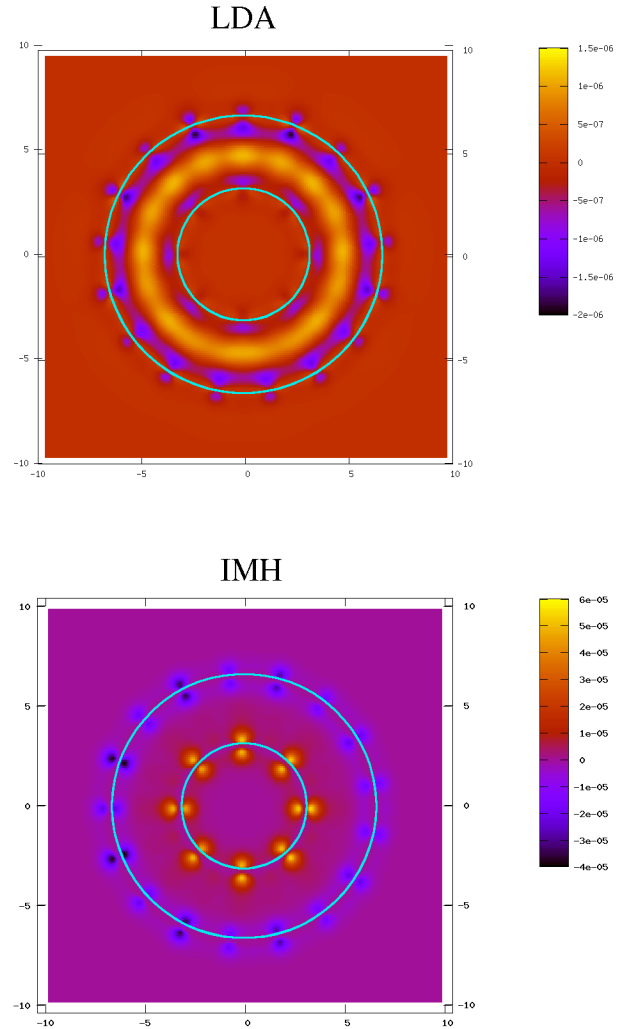


Figure 3: Charge redistribution profile (change of the electron density caused by inter-layer interaction) in the case of the (8,0)@(17,0) DWCNT, in one of the planes perpendicular to the tube axis containing the atoms (units are electrons per \AA^3). The LDA results also agree well with previous calculations³¹, while the IMH results show a more localized redistribution profile owing to the neglect of $s - p$ mixing (see text).

Finally, in order to make a further comparison between the LDA and IMH results, we have calculated the charge redistribution profile using IMH as well. As mentioned above, the LDA results for the (8,0)@(17,0) are in good agreement with previous calculations³¹.

Our results are plotted in Figures 3 and 4, showing the comparison between IMH and LDA in the case of the (8,0)@(17,0) and (6,6)@(11,11) DWCNTs. The IMH model shows a different redistribution profile than the LDA calculation, showing a picture that the electrons deplete from the outer tube and accumulate on the inner wall. This result shows, that while the IMH model fails to

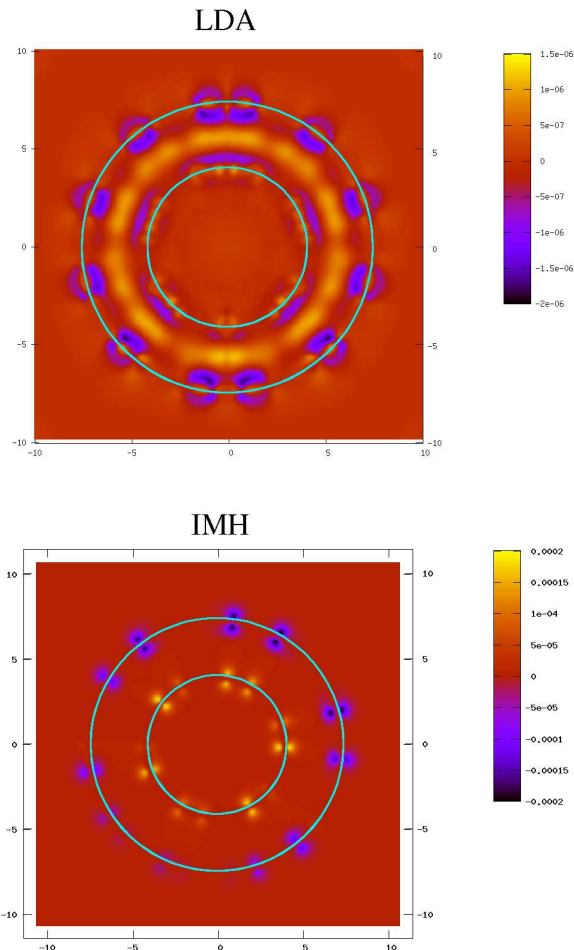


Figure 4: Charge redistribution profile (change of the electron density caused by inter-layer interaction) in the case of the (6,6)@(11,11) DWCNT, in one of the planes perpendicular to the tube axis containing the atoms (units are electrons per \AA^3).

reproduce the correct spatial charge redistribution profile

for this DWCNT, it qualitatively agrees with our result on the direction of the CT. Thus we conclude that proper inclusion of $s - p$ mixing is necessary in order to arrive at the correct spatial distribution of the charge density at small diameters.

V. CONCLUSION

In conclusion, we have performed calculations on a large number of double walled carbon nanotubes, using density functional theory and the inter-molecular Hückel model. We have found that electrons are transferred from the outer tube to the inner tube in all cases, with the magnitude of the average charge transfer density along the tube axis ranging from $0.005 e/\text{\AA}$ to $0.035 e/\text{\AA}$, depending on tube chiralities. We have found that inter-layer orbital mixing is a very important part of the interaction between the layers, and that the interactions can turn a DWCNT consisting of semiconducting subsystems into a metal, but not necessarily in every case. We predict that the majority of metallic DWCNTs have a high density of states at the Fermi level. We have also found that the charge redistribution profile is qualitatively different in the IMH and the LDA calculations due to the neglect of $s - p$ mixing in the former method.

Acknowledgments

We thank O. Dubay and R. Pfeiffer for valuable discussions. Support from OTKA (Grants No. T038014, K60576, T43685, T49718, D45983, TS049881, F61733, and NK60984) in Hungary, the Austrian science foundation (project 17345), and the MERG-CT-2005-022103 EU project is gratefully acknowledged. V. Z. also acknowledges the EU project NANOTEMP BIN2-2001-00580, and F. S. also acknowledges the Zoltán Magyary program.

- ¹ L. X. Benedict, V. H. Crespi, S. G. Louie, and M. L. Cohen, *Phys. Rev. B* **52**, 14935 (1995).
- ² H. Ishii, H. Kataura, H. Shiozawa, H. Yoshioka, H. Otsubo, Y. Takayama, T. Miyahara, S. Suzuki, Y. Achiba, M. Nakatake, et al., *Nature* **426**, 540 (2003).
- ³ D. Connétable, G.-M. Rignanese, J.-C. Charlier, and X. Blase, *Phys. Rev. Lett.* **94**, 015503 (2005).
- ⁴ S. Reich, C. Thomsen, and J. Maultzsch, *Carbon Nanotubes* (Wiley-VCH Verlag GmbH & Co. KGaA, Berlin, 2004).
- ⁵ S. Bandow, M. Takizawa, K. Hirahara, M. Yudasaka, and S. Iijima, *Chem. Phys. Lett.* **337**, 48 (2001).
- ⁶ R. Pfeiffer, H. Kuzmany, C. Kramberger, C. Schaman, T. Pichler, H. Kataura, Y. Achiba, J. Kürti, and V. Zólyomi,

- Phys. Rev. Lett.* **90**, 225501 (2003).
- ⁷ P. M. Singer, P. Wzietek, H. Alloul, F. Simon, and H. Kuzmany, *Phys. Rev. Lett.* **95**, 236403 (2005).
- ⁸ V. Zólyomi and J. Kürti, *Phys. Rev. B* **70**, 085403 (2004).
- ⁹ R. Pfeiffer, F. Simon, H. Kuzmany, and V. N. Popov, *Phys. Rev. B* **72**, 161404 (2005).
- ¹⁰ A. Lázár, P. Surján, M. Paulsson, and S. Stafström, *Int. J. Quantum Chem.* **84**, 216 (2002).
- ¹¹ P. Surján, A. Lázár, and Á. Szabados, *Phys. Rev. A* **68**, 062503 (2003).
- ¹² V. Zólyomi, Á. Ruzsnyák, J. Kürti, Á. Gali, F. Simon, H. Kuzmany, Á. Szabados, and P. R. Surján, *phys. stat. sol. (b)* **243**, 3476 (2006).
- ¹³ H. Shiozawa et al, to be published.

- ¹⁴ G. Kresse and J. Furthmüller, Phys. Rev. B **54**, 11169 (1996).
- ¹⁵ P. Ordejón, E. Artacho, and J. M. Soler, Phys. Rev. B **53**, 10441 (1996).
- ¹⁶ L. Henrard, E. Hernández, and A. Rubio, Phys. Rev. B **60**, 8521 (1999).
- ¹⁷ Y.-K. Kwon and D. Tománek, Phys. Rev. Letters **84**, 1483 (2000).
- ¹⁸ Y.-K. Kwon and D. Tománek, Phys. Rev. B **58**, R16001 (1998).
- ¹⁹ A. Palsler, Phys. Chem. Chem. Phys. **1**, 4459 (1999).
- ²⁰ S. Tabor and S. Stafstrom, Journal of Magnetism and Magnetic Materials **104**, 2099 (1992).
- ²¹ S. Stafström, Phys. Rev. B **47**, 12437 (1993).
- ²² M. Paulsson and S. Stafström, Phys. Rev. B **60**, 7939 (1999).
- ²³ Á. Szabados, L. Biró, and P. Surján, Phys. Rev. B **73**, 195404 (2006).
- ²⁴ H. C. Longuet-Higgins and L. Salem, Proc. Royal. Soc. **A251**, 172 (1959).
- ²⁵ M. Kertész and P. R. Surján, Solid State Communications **39**, 611 (1981).
- ²⁶ J. Kürti, V. Zólyomi, M. Kertesz, and G. Sun, New J. Phys. **5**, 125 (2003).
- ²⁷ Á. Ruzsnyák, V. Zólyomi, J. Kürti, S. Yang, and M. Kertesz, Phys. Rev. B **72**, 155420 (2005).
- ²⁸ G. Henkelman, A. Arnaldsson, and H. Jónsson, Comput. Mater. Sci. **36**, 254 (2006).
- ²⁹ Y. Miyamoto, S. Saito, and D. Tomanek, Phys. Rev. B **65**, 041402(R) (2002).
- ³⁰ S. Okada and A. Oshiyama, Phys. Rev. Lett. **91**, 216801 (2003).
- ³¹ B. Shan and K. Cho, Phys. Rev. B **73**, 081401(R) (2006).